International Journal of Mechanical Engineering and Technology (IJMET)
Volume 9, Issue 5, May 2018, pp. 1011–1021, Article ID: IJMET_09_05_112
Available online at http://www.iaeme.com/ijmet/issues.asp?JType=IJMET&VType=9&IType=5
ISSN Print: 0976-6340 and ISSN Online: 0976-6359

VIBRATION ANALYSIS OF TEMPERATURE-DEPENDENT FG-CNT REINFORCED COMPOSITE PLATES

Shubham Abhinav Soni, Nishant Mundeja, Swaroop ANSP, Benedict Thomas
School of Mechanical Engineering, VIT University, Vellore, Tamil Nadu

ABSTRACT

The application of functionally graded materials (FGMs) has drastically increased in distinct fields of engineering. In the recent past Carbon nanotube (CNT) reinforced composite has gained significant importance in the material engineering community as a replacement to the conventional FRP composites. This paper deals with the vibration analysis of temperature dependent functionally graded carbon nanotube reinforced composites (FG-CNTRCs). Various types of distributions of single walled carbon nanotubes (SWCNTs) are considered and the material properties of functionally graded carbon nanotube-reinforced composites (FG-CNTRCs) are assumed to be graded through the thickness direction of carbon nanotubes. In the present work free vibration analysis is performed to study the effect of temperature and CNT distribution on natural frequencies of the CNTRC plate. Comparative results for various types of CNTRC plates have also been presented. The results show that CNT distribution and temperature have substantial effect on the vibration characteristics of the FG-CNTRC plate.

Keywords: CNT, Free Vibration, Functionally Graded, Temperature Dependent

Cite this Article: Shubham Abhinav Soni, Nishant Mundeja, Swaroop ANSP, Benedict Thomas, Vibration Analysis of Temperature-Dependent FG-CNT Reinforced Composite Plates, International Journal of Mechanical Engineering and Technology, 9(5), 2018, pp. 1011–1021.
http://www.iaeme.com/IJMET/issues.asp?JType=IJMET&VType=9&IType=5

1. INTRODUCTION

Carbon nanotubes exhibits outstanding thermal, mechanical and electrical properties and are ominously used as a reinforcement material for high performance structural composites with sizeable application potentials fields like automotive, aerospace, locomotive etc. Known for advanced mechanical properties such as light weight, high stiffness and high strength, carbon nanotubes are applied in layers in innovative laminated structures. However, since in traditional composites reinforcement is distributed either uniformly or randomly throughout, the mechanical properties do not vary spatially at the macroscopic level. But, functionally graded materials are composite materials whose properties vary spatially according to a certain non-uniform distribution of the reinforcement. Functionally graded materials (FGMs),

composed of metal and ceramic typically, have been widely used in many engineering applications and working environments, especially in high temperature and large temperature gradient environments. Stimulated by the concept of functionally graded materials, the functionally graded distribution methodology has been applied to CNT-reinforced functionally graded materials. Since FGMs have many advantages, a number of investigations dealing with thermal behaviors of functionally graded plates and shells were published in scientific literature, such as static and transient thermo- elastic responses, nonlinear free flexural vibrations in thermal environments, and thermal post buckling behaviors with temperature-independent material properties and with temperature- dependent properties.

Andrews R, Weisenberger MC [1] demonstrated that a carbon nano tube polymer composite have excellent mechanical properties since they do not break and remain straight after the cutting process, which involves cutting thin slices (50-200 nanometers) of the composite material. Zhou G, Duan W, Gu B [2] studied the morphology and mechanical properties of single walled carbon nanotubes (SWCNT) by using first principles cluster method within the framework of local density approximation. They used HRTEM images to show that the nano-tubes have honeycomb structure and the tensile strength of carbon nanotube (6.249 GPa) is greater than that of carbon fiber (2.6 GPa), but less than the in-plane tensile strength of graphite(20 GPa). This proves the high strength of carbon nano tubes. Fidelus JD, Wiesel E, Gojny FH, Schulte K, Wagner HD [3] explored the thermo-mechanical properties of epoxy based nano-composites having low weight fractions of randomly oriented single and multi-walled carbon nanotubes. Elastic modulus by dynamic mechanical thermal analysis and toughness under tensile impact using notched specimens were examined. Both the properties were improved by adding a very little nanotube weight fraction. However, the tensile impact toughness was significantly increased by 18 to 35%. Schapery RA [4] ascertained the upper and lower limits on thermal expansion coefficients of transversely isotropic composite material with two phase and three phase systems. He also devised explicit formulas for linear expansion coefficient and volumetric expansion coefficient of elastic and visco-elastic materials. Mirzaei M, Kiani Y [5] contrived an aboveboard method to achieve the deflection in lateral direction as a function of raised temperature for a beam with both edges fixed. They corroborated that by establishing a proper distribution of CNT's, the critical buckling temperature of an FG-CNT has enhanced. Shen HS [6] excogitated the post buckling analysis in thermal environment of CNTRC shells subjects to axial compression. The material properties were obtained from molecular dynamics (MD) simulations. The governing equations were based on a higher order shear deformation shell theory using Kármán-type of kinematic nonlinearity and contained thermal effects. Zhang LW, Zhu P, Liew KM [7] contrived the local Krigingmeshless to investigate the buckling analysis of FG-CNT under the mechanical and thermal loadings based on the first order shear deformation plate theory involving transverse shear strains of FC-CNT. They studied the influence of volume fraction exponent, boundary condition, length-to-thickness ratios and loading types on the buckling behaviors of FG-CNT. Yang J, Liew KM, Wu YF, Kitipornchai S [8] conducted the thermo-mechanical post-buckling analysis of cylindrical panels that are made of functionally graded materials (FGMs) with temperature-dependent thermo-elastic properties that are graded in the direction of thickness according to a simple power law distribution in terms of the volume fractions of the constituents. Wu Lanhe [9] established the analytical solution of the equations for the first order shear deformation theory considering the thermal loading, uniform temperature rise and gradient through the thickness. Reddy JN, Liu CF [10] examined the thermo elasto-dynamic and static response of plates subjected to pressure loading and thickness varying temperature fields. The thickness variation of the temperature field comes about also due to the dissimilarity of the thermal properties. Zenkour AM, Sobhy M [11] has

discussed the thermal buckling analysis of functionally graded material (FGM) plates resting on two-parameter Pasternak's foundations is investigated. Equilibrium and stability equations of FGM plates were derived based on the trigonometric shear deformation plate theory and includes the plate foundation interaction and thermal effects. Hiroyuki Matsunaga [12] presented a two-dimensional global higher-order deformation theory for thermal buckling of cross-ply laminated composite and sandwich plates. By using the method of power series expansion of continuous displacement components, a set of fundamental governing equations taken into the account, the effects of both transverse shear and normal stresses is derived through the principle of virtual work. Amy M. Marconnet [13] discussed the effect of CNT density on thermal conduction in view of boundary resistances, increased defect concentrations, and the possibility of suppressed phonon modes in the CNTs. Zhu P, Lei ZX, Liew KM [14] presented the free vibration analysis and bending analysis of thin-to-moderately thick composite plates reinforced along single-walled carbon nano-tubes utilizing the finite element method on the grounds of first order shear deformation plate theory. James Elliott, Han Y [15] presented classical molecular dynamics (MD) simulations of model polymer/CNT composites retraced by imbedding a single wall (10, 10) CNT into two unlike amorphous polymer matrices: Poly (methyl methacrylate) (PMMA) and poly {(m-phenylenevinylene)-co- [(2,5-dioctoxy-p-phenylene) vinylene]} (PmPV), respectively, with dissimilar volume fractions.

This paper deals with the vibration analysis of temperature dependent FG-CNTRC plate under clamped condition. Comparative studies have been carried out to verify the accuracy of the present method for analysis of free vibration of various types of CNTRC plates.

2. MATERIAL MODELLING

We have considered a composite material, Poly (methyl methacrylate) PMMA is taken as matrix, which is assumed to be isotropic in nature and it is reinforced with SWCNT. The distribution of CNT can be uniformly (UD) or functionally graded (FG) in thickness direction as shown in Fig1. The length, width and total thickness of the CNTRC plate are b, a, and h. It is assumed that the coordinate system has its origin at the corner of the plate on the middle plane Z (–h/2 to h/2)is perpendicular to the plate. Z ranges from.

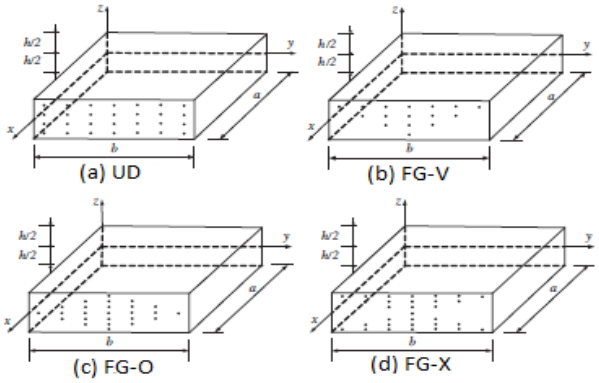

Figure 1 Distribution of CNTRC plates. (a) UD; (b) FG-V; (c) FG-O; (d) FG-X.

There can be five types of CNTRC plates, UD-CNTRC represents the uniform distribution and FG-V, FG-O and FG-X CNTRC the functionally graded distributions of carbon nanotubes in the composite plates. Several micromechanical models have been developed to predict the effective material properties of the mixture of reinforcement and matrix e.g. Mori–Tanaka scheme [12] and the rule of mixture [3]. For nanoparticles mixture,

the Mori–Tanaka scheme and the rule of mixture is applicable. The rule of mixture is a simple and convenient way for predicting the overall material properties and responses of the structures

The rule of mixture was employed by introducing the CNT efficiency parameters and the effective material properties of CNTRC plates can thus be written as [3]

$$\begin{aligned} &E_{11}=h_1 V_{cnt} E_{11}^{cnt}+V_m E_m \ , \\ &\frac{h_2}{E_{22}}=\frac{V_{cnt}}{E_{22}^{cnt}}+\frac{V_m}{E_m} \ , \\ &\frac{h_3}{G_{12}}=\frac{V_{cnt}}{G_{12}^{cnt}}+\frac{V_m}{G_m} \end{aligned} \tag{1}$$

Where, $E_{11}^{cnt}, E_{22}^{cnt}$ and G_{12}^{cnt} indicate the Young's moduli and shear modulus of SWCNTs, respectively, and E_m and G_m represent the corresponding properties of the matrix. The introduction of h_j (j = 1, 2, 3), the CNT efficiency parameters, was to consider size-dependent property. The efficiency parameters can be obtained by matching the effective properties of CNTRC from MD simulations with the rule of mixture.

The CNT volume fractions V_{cnt} of various types of FG-CNTRC beam is written as:

$$V_{cnt}=\begin{cases} V_{cnt}^{*} & (\text{UD CNTRC}), \\ \left(1-\dfrac{2|z|}{h}\right)V_{cnt}^{*} & (\text{FG-V CNTRC}), \\ \dfrac{4|z|}{h}V_{cnt}^{*} & (\text{FG-X CNTRC}), \\ 2\left(1-\dfrac{2|z|}{h}\right)V_{cnt}^{*} & (\text{FG-O CNTRC}), \end{cases} \tag{2}$$

$$V_{cnt}^{*}=\frac{w_{cnt}}{w_{cnt}+\dfrac{\rho_{cnt}}{\rho_m}-\left(\dfrac{\rho_{cnt}}{\rho_m}\right)w_{cnt}} \tag{3}$$

where, w_{cnt} is the mass fraction of nanotube, and ρ_{CNT} and ρ_m are the densities of carbon nanotube and matrix, respectively. For this linear material property variation, material properties may be obtained by substituting the value of V_{cnt} in equation (1).

Since Poisson's ratio depends weakly on the position, we assume u_{12} to be:

$$\upsilon_{12}=V_{cnt}^{*}\upsilon_{12}^{cnt}+V_m\upsilon_m \tag{4}$$

In addition, V_{cnt} and V_m are the volume fractions of the CNTs and the matrix, which satisfy the relationship of

$$V_{cnt}+V_m=1 \tag{5}$$

Similarly, mass density ρ is calculated by:

$$\rho=\rho_{cnt}V_{cnt}+\rho_m V_m \tag{6}$$

where, ρ_{CNT} and ρ_m are the, mass density of the CNTs and the matrix, respectively. The Poisson's ratio and density of CNT and matrix depends weakly on change in temperature and therefore are taken as constant with respect to temperature.

3. EQUATION OF MOTION

The dynamic finite element formulation has been derived by using the equation of motion, for elements it can be written as

$$\left[M_{uu}^{e}\right]\left\{\ddot{d}^{e}\right\}+\left[K_{uu}^{e}\right]\left\{d^{e}\right\}=\left\{F^{e}\right\} \tag{7}$$

The equation of motion of whole structure can be represented as

$$[M]\left\{\ddot{d}\right\}+[C]\left\{\dot{d}\right\}+[K]\{d\}=\{F\} \tag{8}$$

For free vibration analysis, the equation (8) can be reduced by neglecting damping and external forces to

$$[M]\left\{\ddot{d}\right\}+[K]\{d\}=\{0\} \tag{9}$$

Eigenvalue problem of the system can be written as:

$$\left([K]-\omega^{2}[M]\right)\{X\}=0 \tag{10}$$

where, ω^2 is the eigenvalue and X is the eigenvector of the system.

4. RESUTS AND DISUSSION

Table 1 Comparison of results for width-to-thickness ratio (b/h=50) and different CNT volume fraction on the non–dimensional natural frequency ($\overline{\omega}$) for CNTRC square plates (CCCC). Where

$$\overline{\omega}=\omega_{mn}\frac{a^{2}}{h}\sqrt{\frac{\rho_m}{E_m}}$$

V_{CNT}	Modes (m,n)	UD		FG-X	
		Zhu [14]	ANSYS (Present)	Zhu [14]	ANSYS (Present)
0.11	(1,1)	39.730	39.391	46.166	45.291
	(1,2)	43.876	43.433	49.934	49.011
	(1,3)	54.768	53.628	60.225	58.709
	(1,4)	74.488	71.289	79.534	76.036
	(2,1)	98.291	96.057	108.694	100.853
	(2,2)	100.537	96.666	110.921	108.406
0.14	(1,1)	43.583	43.222	50.403	49.443
	(1,2)	47.479	47.032	54.025	53.019
	(1,3)	57.968	56.866	64.112	62.522
	(1,2)	77.395	74.267	83.394	79.798
	(2,1)	106.371	99.033	112.896	104.852
	(2,2)	106.487	104.689	119.134	116.320
0.17	(1,1)	49.074	48.620	57.245	55.864
	(1,2)	54.324	53.728	62.236	60.774
	(1,3)	68.069	66.582	75.746	73.488
	(1,4)	92.868	88.772	100.850	95.992
	(2,1)	121.669	119.524	137.913	127.981
	(2,2)	124.518	119.824	138.485	133.700

Table 1 shows the non-dimensional natural frequency ω̃ for uniform distributed (UD) and X functionally graded CNTRC (FG-V, FG-O and FG-X) for width-to-thickness ratio (b/h=50) subjected to clamped boundary conditions (CCCC). It can be seen from the table that the ANSYS results from the proposed approach are in a good agreement with the published literature results.

Table 2 Effect of temperature dependent properties on natural frequencies for fundamental modes for Vcnt= 12%

Temperature (K)	Modes (m,n)	UD	FG-O	FG-X	FG-V
300	(1,1)	1692.1	1283.6	1936.7	2061
	(1,2)	1909	1556.5	2138.8	2254.8
	(1,3)	2447.3	2175.6	2657.7	2760.5
	(1,4)	3351.7	3144.7	3555.2	3649.1
	(2,1)	4109.2	3187.6	4584.7	4836.8
	(2,2)	4229.6	3346.6	4695.2	4900.7
500	(1,1)	1606.6	1223.2	1824.5	1936.2
	(1,2)	1772.9	1433.8	1980.2	2085.6
	(1,3)	2200	1931.4	2391.9	2486.9
	(1,4)	2940.1	2733.5	3124.8	3211.6
	(2,1)	3825	3005.3	4166.3	4252.5
	(2,2)	3916.3	3125.3	4219.1	4434.2
700	(1,1)	1480.6	1143.1	1655.1	1746.7
	(1,2)	1592.9	1285.3	1761.4	1849.2
	(1,3)	1894.5	1640.7	2053.8	2134.6
	(1,4)	2440.7	2241.4	2595	2669.7
	(2,1)	3227.1	2737.2	3386.8	3460.3
	(2,2)	3398.8	2816.1	3680.9	3846.1
1000	(1,1)	733.44	642.38	756.34	778.58
	(1,2)	755.79	667.59	779.42	801.47
	(1,3)	822.94	741.62	848.91	870.61
	(1,4)	959.22	887.95	989.83	1011.5
	(2,1)	1175.3	1114	1212.9	1235.5
	(2,2)	1468.7	1308.6	1506.4	1540.3

Table 3 Effect of temperature dependent properties on natural frequencies for fundamental modes for Vcnt= 17%

Temperature (K)	Modes (m,n)	UD	FG-O	FG-X	FG-V
300	(1,1)	2065.1	1560.8	2371.1	2534
	(1,2)	2360.2	1931.5	2655.8	2809.9
	(1,3)	3079.9	2754.8	3372	3515.4
	(1,4)	4270.5	3898	4585.6	4729.3
	(2,1)	5057.8	4024.7	5660	6021.6
	(2,2)	5222.8	4116.4	5816.4	6171.8
500	(1,1)	1967.6	1492.2	2245.2	2392.1
	(1,2)	2193.7	1778.3	2463.8	2604.4
	(1,3)	2765.2	2441.1	3031.3	3164.2
	(1,4)	3740.9	3494.1	4022.1	4155.8
	(2,1)	4733.3	3698.4	5244.4	5554.1
	(2,2)	4857.8	3862.6	5363.7	5560
700	(1,1)	1825.1	1403.4	2045.9	2176.6
	(1,2)	1977.2	1596.1	2195	2321.4
	(1,3)	2380.6	2070.3	2598.9	2718.7
	(1,4)	3101.5	2860.4	3333.8	3451.1
	(2,1)	4129.8	3403.5	4394.1	4519
	(2,2)	4240.6	3510.8	4596.4	4860.2
1000	(1,1)	935.25	825.37	960.12	1004.9
	(1,2)	964.54	858.23	991.69	1036.1
	(1,3)	1052.3	954.46	1086.1	1130
	(1,4)	1229.8	1144.3	1276.1	1320.1
	(2,1)	1510.4	1437.4	1574.3	1620.6
	(2,2)	1879.3	1695.9	1914.6	2002.3

Table 4 Effect of temperature dependent properties on natural frequencies for fundamental modes for Vcnt=28%

Temperature (K)	Modes (m,n)	UD	FG-O	FG-X	FG-V
300	(1,1)	2479.4	1893.4	2803.2	3029.8
	(1,2)	2748.4	2216.1	3097.4	3325.1
	(1,3)	3435.2	2980	3856.3	4096.2
	(1,4)	4617.9	4215	5166.5	5444
	(2,1)	5933.6	4723.2	6463.7	7021
	(2,2)	6080.6	4906.3	6623.8	7180.1
500	(1,1)	2345.9	1812.9	2619.2	2836
	(1,2)	2552.4	2060.1	2847.5	3064.8
	(1,3)	3096.4	2668.4	3453.5	3678.9
	(1,4)	4061.4	3683.8	4527.8	4781.4
	(2,1)	5430.5	4463.7	5891.4	6355.2
	(2,2)	5488.6	4601.1	6015.5	6409.8
700	(1,1)	2143.5	1701.3	2340.2	2540.9
	(1,2)	2283.7	1866.7	2498.7	2699.2
	(1,3)	2668.3	2295.9	2934.6	3139.3
	(1,4)	3379.3	3048	3735.2	3958
	(2,1)	4418.8	4069.6	4896.3	5157.9
	(2,2)	4823.9	4107.3	5066.6	5524.3
1000	(1,1)	1008.3	948.42	1005.1	1100.7
	(1,2)	1037.8	977.72	1042.2	1137.4
	(1,3)	1126.9	1065.5	1152.6	1247.6
	(1,4)	1308.5	1243.6	1371.6	1469.1
	(2,1)	1597.8	1526.3	1710.2	1815.8
	(2,2)	1991.6	1910.9	1995.4	2186.6

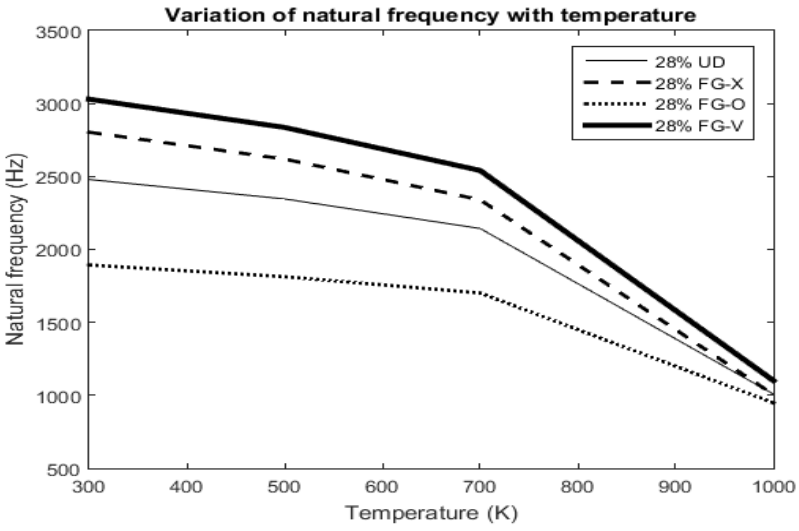

Figure 2 Comparison of natural frequencies of UD & FG-CNT with varying temperature at volume fraction of 28% CNT.

The free vibration mode shapes of a CCCC CNTRC plate for volume fraction of 28% CNT, at 1000K are shown in the following pages.

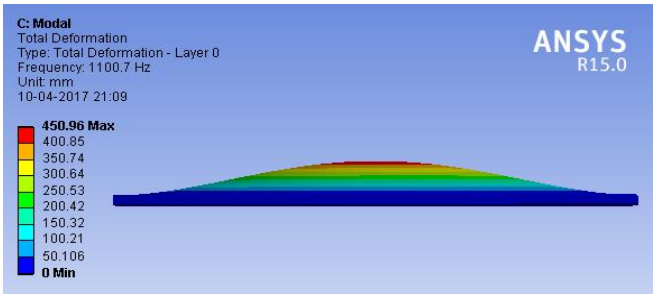

(a) 1st Mode

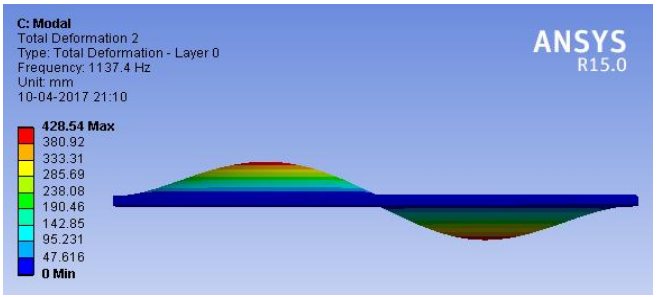

(b) 2nd Mode

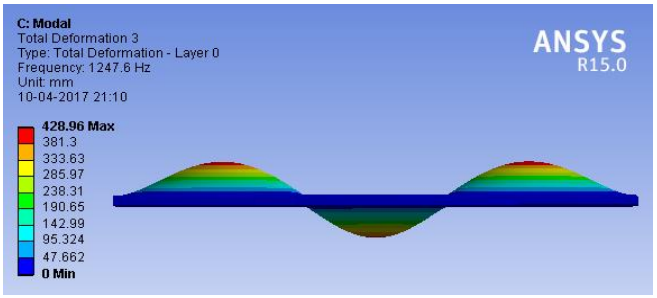

(c) 3rd Mode

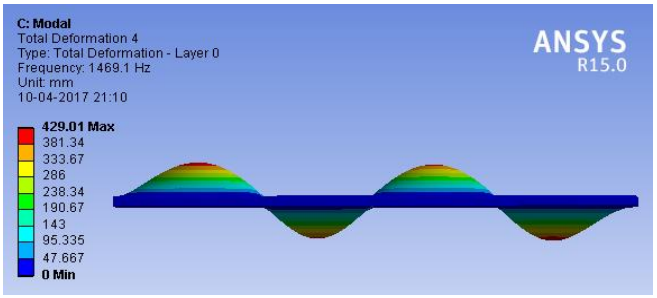

(d) 4th Mode

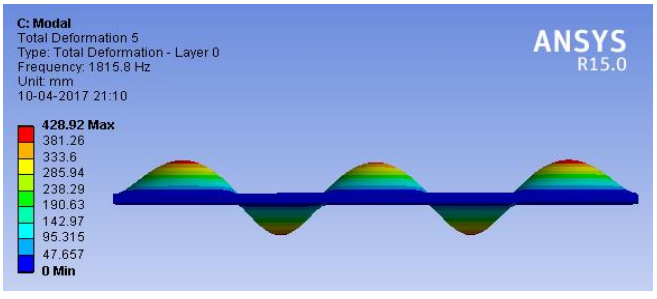

(e) 5th Mode

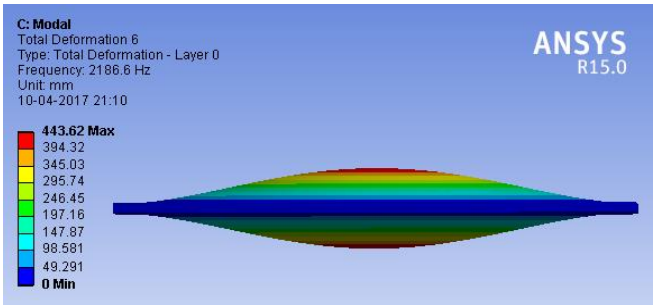

(f) 6th Mode

Figure 3 The free vibration mode shapes of a CCCC CNTRC plate 28% CNT, at 1000K. (a) 1st Mode; (b) 2nd Mode; (c) 3rd Mode; (d) 4th Mode; (e) 5th Mode; (f) 6th Mode.

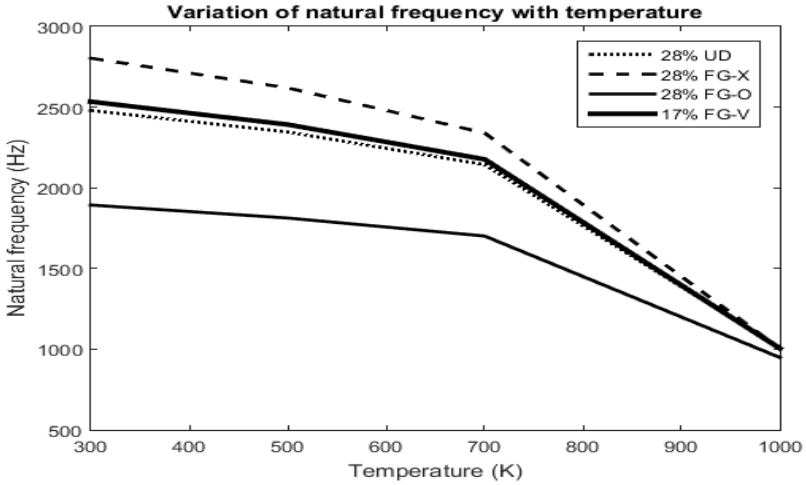

Figure 4 Comparison of natural frequencies of volume fraction 17% FG-V with volume fraction 28% UD and FG CNT(FG-X, FG-O) at different temperatures.

Numerical results are presented in this section for geometrically mid-plane symmetric FG-CNTRC plates subjected to in-plane temperature variation. Poly methyl methacrylate (PMMA) [15] is considered as the matrix, the material properties of which are assumed to be, ρ_m=1.15 g/cm^3 and E_m=(3.52-0.0034T) GPa, in which $T = T_\circ + \Delta T$ and at $T_\circ = 300K$ (room temperature). Therefore at $T = 300K$, E_m=2.5 GPa. We have chosen the armchair (10, 10) SWCNTs as the reinforcements. The CNT efficiency parameter h_j introduced in through Eq. (1) were determined by Zhang and Shen according to the effective properties of CNTRCs available (e.g. in [6]) by matching the Young's moduli E11 and E22 with the counterparts computed by the rule of mixture given in the table. In addition, we assume that $h_2 = 0.7h_3$, $G_{12} = G_{13}$ and $G_{23} = 1.2G_{12}$. Other iterations are obtained by following this procedure.

*Free Vibration: T*he width-to-thickness ratios (b/h) of the plates are considered as 50, and the thickness as 2.0 mm. We have considered four types of square plates (a/b = 1), UD-CNTRC, FG-V, FG-O and FG-X CNTRC, with boundary conditions as all edges clamped (CCCC) for different CNT volume fraction (12%, 17% and 28%).

$$u_n = u_s = \omega_o = \varphi_n = \varphi_s = 0 \qquad \text{(Clamped edge)} \qquad (11)$$

From Fig. 2, it is clear that on comparing all the types of plates (UD-CNTRC, FG-X, FG-O and FG-V) with respect to natural frequency, FG-V is giving the best outcome in terms of

highest natural frequency which in turn results in highest stiffness for various CNT volume fractions. We also observed that, as the temperature increases, the natural frequency of the plate decreases resulting in decrease of stiffness.

Fig. 3 shows the first six mode shapes of fundamental frequency for CCCC FG-V CNTRC plate at 28% CNT volume fraction.

The Fig. 4 depicts that the results of FG-V type of CNT distribution at 17% CNT volume fraction provides better results compared to UD and FG-O CNT distribution at 28% volume fraction of CNT. This shows that use of 17% CNT FG-V distribution will be a better alternative to 28% CNT FG-O and UD in terms of stiffness, weight and cost.

5. CONCLUSIONS

In this paper, free vibration analyses of temperature dependent carbon nanotube-reinforced functionally graded composite plates are investigated. The effective material properties of the CNTRC are estimated using the extended rule of mixture. Free vibration analysis is carried out to present the natural frequency of the FG-CNTRC plate. The result obtained in the present analysis shows a very good agreement with those available in literature. It is observed from the results that natural frequencies and vibration mode shapes of the CNTRC plate are highly dependent on the CNT volume fraction and CNT distribution. Also, the temperature change has a significant effect on the stiffness. Hence, material will deform easily under high loading condition subjected to high temperatures. It is also found that FG-V type of distribution gives highest stiffness at even higher temperature when compared to FG-O, FG-X, FG-V and UD- type of distribution of FG-CNTRC.

Finally, it can be concluded that the CNT volume fraction, CNT distribution and temperature has a prominent effect on the dynamic characteristics of the FG-CNTRC plate.

REFERENCES

[1] Andrews R, Weisenberger MC. Carbon nanotube polymer composites. Curr Opin Solid State Mater Sci 2004;8:31–7. doi:10.1016/j.cossms.2003.10.006.

[2] Zhou G, Duan W, Gu B. First-principles study on morphology and mechanical properties of single-walled carbon nanotube 2001;333:344–9.

[3] Fidelus JD, Wiesel E, Gojny FH, Schulte K, Wagner HD. Thermo-mechanical properties of randomly oriented carbon / epoxy nanocomposites 2005;36:1555–61. doi:10.1016/j.compositesa.2005.02.006.

[4] Schapery RA. Thermal Expansion Coefficients of Composite Materials Based on Energy Principles. J Compos Mater 1968;2:380–404. doi:10.1177/002199836800200308.

[5] Mirzaei M, Kiani Y. Nonlinear free vibration of temperature-dependent sandwich beams with carbon nanotube-reinforced face sheets. Acta Mech 2016;227:1869–84. doi:10.1007/s00707-016-1593-6.

[6] Shen HS. Postbuckling of nanotube-reinforced composite cylindrical shells in thermal environments, Part I: Axially-loaded shells. Compos Struct 2011;93:2096–108. doi:10.1016/j.compstruct.2011.02.011.

[7] Zhang LW, Zhu P, Liew KM. Thermal buckling of functionally graded plates using a local Kriging meshless method. Compos Struct 2014;108:472–92. doi:10.1016/j.compstruct.2013.09.043.

[8] Yang J, Liew KM, Wu YF, Kitipornchai S. Thermo-mechanical post-buckling of FGM cylindrical panels with temperature-dependent properties. Int J Solids Struct 2006;43:307–24. doi:10.1016/j.ijsolstr.2005.04.001.

[9] Lanhe W. Thermal buckling of a simply supported moderately thick rectangular FGM plate. Compos Struct 2004;64:211–8. doi:10.1016/j.compstruct.2003.08.004.

[10] Reddy JN, Liu CF. A higher-order shear deformation theory of laminated elastic shells. Int J Eng Sci 1985;23:319–30. doi:10.1016/0020-7225(85)90051-5.

[11] Zenkour AM, Sobhy M. Thermal Buckling of Functionally Graded Plates Resting On Elastic Foundations Using the Trigonometric Theory. J Therm Stress 2011;34:1119–38. doi:10.1080/01495739.2011.606017.

[12] Matsunaga H. Thermal buckling of cross-ply laminated composite and sandwich plates according to a global higher-order deformation theory. Compos Struct 2005;68:439–54. doi:10.1016/j.compstruct.2004.04.010.

[13] Published A, Link C, Terms D. Thermal Conduction in Aligned Carbon Nanotube-Polymer Nanocomposites with High Packing Density 2015:4818–25.

[14] Zhu P, Lei ZX, Liew KM. Static and free vibration analyses of carbon nanotube-reinforced composite plates using finite element method with first order shear deformation plate theory. Compos Struct 2012;94:1450–60. doi:10.1016/j.compstruct.2011.11.010.

[15] Han Y, Elliott J. Molecular dynamics simulations of the elastic properties of polymer/carbon nanotube composites. Comput Mater Sci 2007;39:315–23. doi:10.1016/j.commatsci.2006.06.011.

[16] M. Karthick, M.Sundarraj and T.Raja, Vibration Analysis of Coated Spur Gears, International Journal of Mechanical Engineering and Technology 9(2), 2018. pp. 409 – 416

[17] Priyatham Dakuri and Hari Sankar Vanka, Vibration Analysis Of Isotropic And Composite Stiffened Pressure Hulls Under Initial Stress. International Journal of Design and Manufacturing Technology 9(1), 2018, pp. 1–7.